ISCI, Volume 7

Supplemental Information

Fundamental Characteristics of Single-Cell Aging in Diploid Yeast

Ethan A. Sarnoski, Ruijie Song, Ege Ertekin, Noelle Koonce, and Murat Acar

SUPPLEMENTAL FIGURES

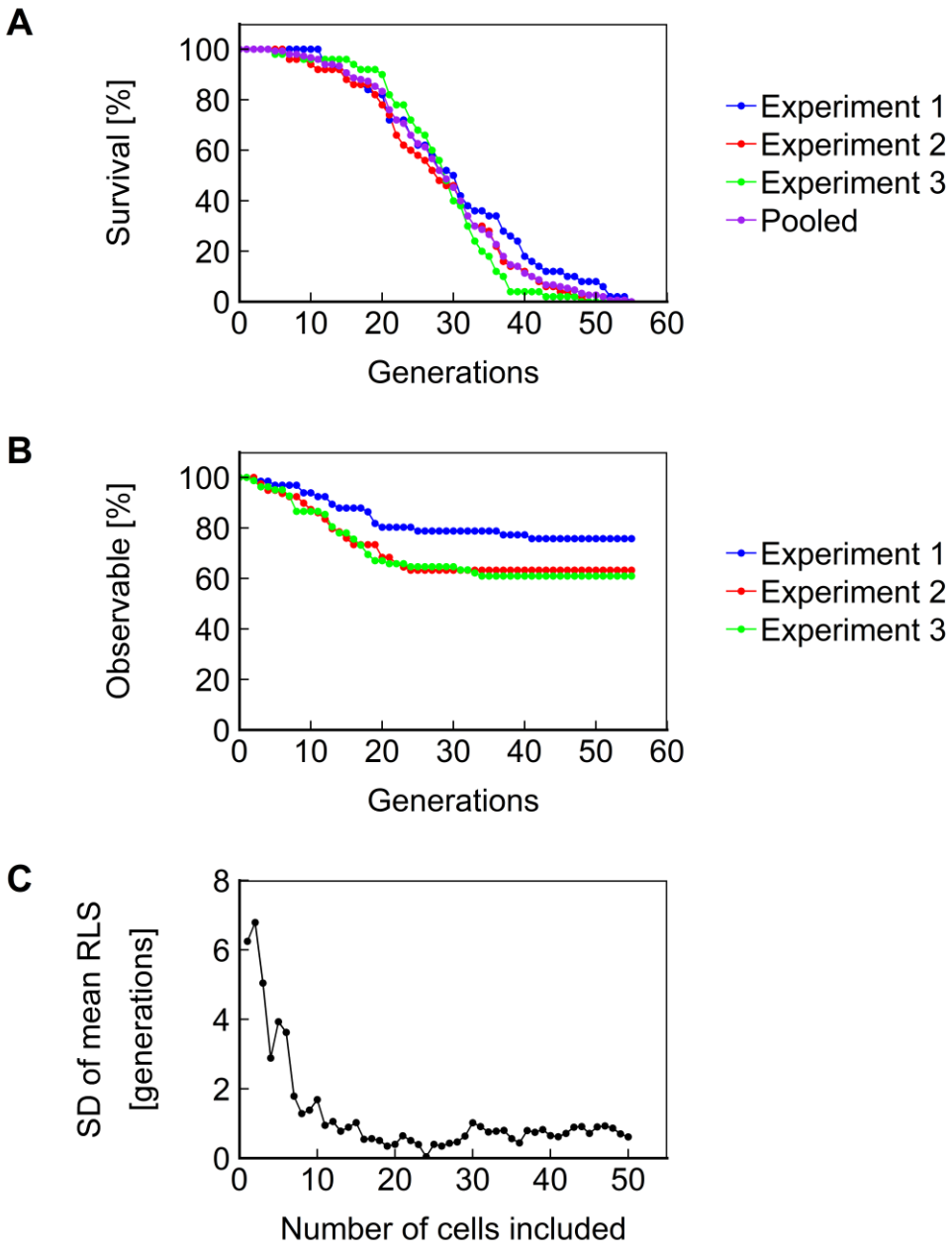

Figure S1. Validation of the Duplicator. Related to Figure 1. A. Survival curves of 50 cells each for three independent experiments performed using the wild-type BY4743 strain, and a pooled survival curve combining all 150 cells. **B.** Retention of cells in the experiments shown in (**A**), showing the fraction of cells that entered a trap and budded at least once prior to the 12th hour of the experiment, and remained within the field-of-view until a given age. **C.** Standard deviation of mean replicative lifespan calculated as a function of the number of cells included in the calculation.

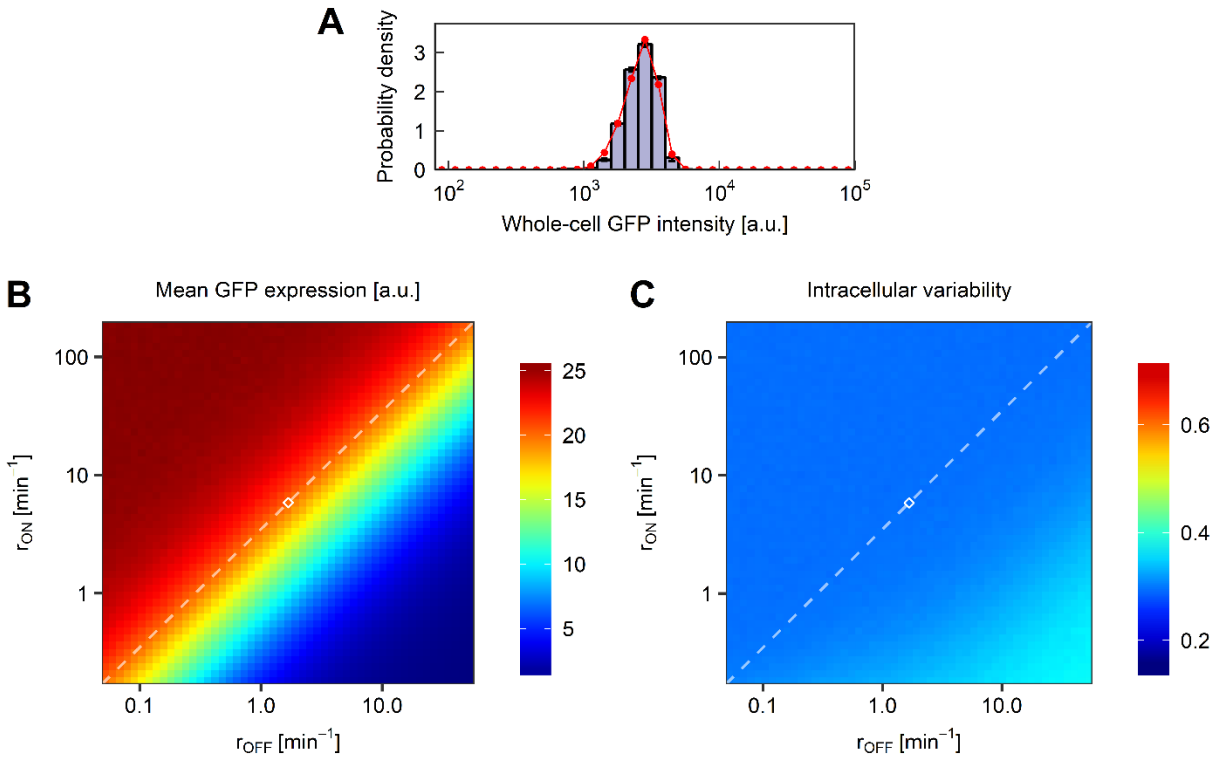

Figure S2. Model results for the heterozygous P_{TEF1}-ssGFP at *SAM2* locus strain. Related to Figure 4. **A.** Comparison of fit results (red) and experimental data for the heterozygous P_{TEF1}-ssGFP at *SAM2* locus strain. Error bars indicate s.e.m. (N=2). **B-C.** Effects of changes in r_{ON} and r_{OFF} on the mean expression level (**B**) and intracellular variability as measured by the coefficient of variation (**C**). White diamond indicates the fitted r_{ON} and r_{OFF} values. Dashed line indicates the result of simultaneous changes in r_{OFF} and r_{ON}.

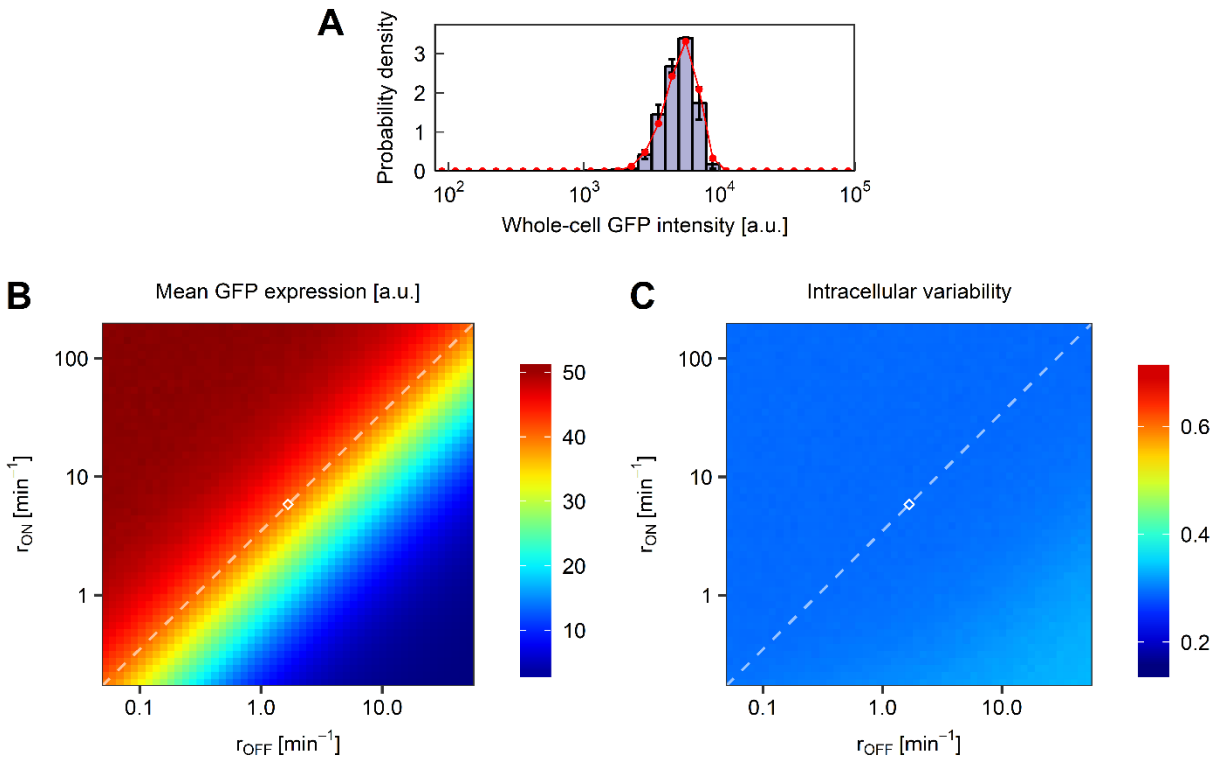

Figure S3. Model results for the homozygous P_{TEF1}-ssGFP at *SAM2* locus strain. Related to Figure 5. **A.** Comparison of simulation results (red) and experimental data for the homozygous P_{TEF1}-ssGFP at *SAM2* locus strain. Error bars indicate s.e.m. (N=2). **B-C.** Effects of changes in r_{ON} and r_{OFF} on the mean expression level (**B**) and intracellular variability as measured by the coefficient of variation (**C**). White diamond indicates the fitted r_{ON} and r_{OFF} values. Dashed line indicates the result of simultaneous changes in r_{OFF} and r_{ON}.

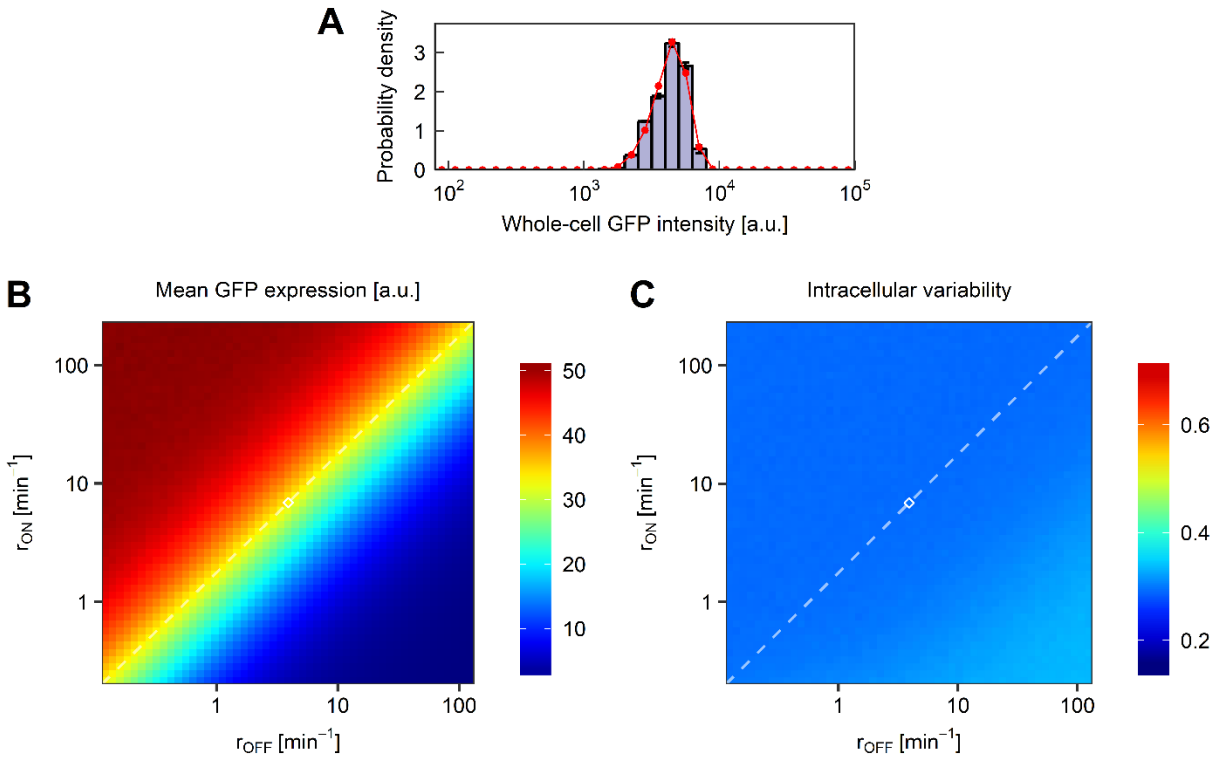

Figure S4. Model results for the homozygous P_{TEF1}-ssGFP at *HIS3* locus strain. Related to Figure 6. **A.** Comparison of fit results (red) and experimental data for the homozygous P_{TEF1}-ssGFP at *HIS3* locus strain. Error bars indicate s.e.m. (N=2). **B-C.** Effects of changes in r_{ON} and r_{OFF} on the mean expression level (**B**) and intracellular variability as measured by the coefficient of variation (**C**). White diamond indicates the fitted r_{ON} and r_{OFF} values. Dashed line indicates the result of simultaneous changes in r_{OFF} and r_{ON}.

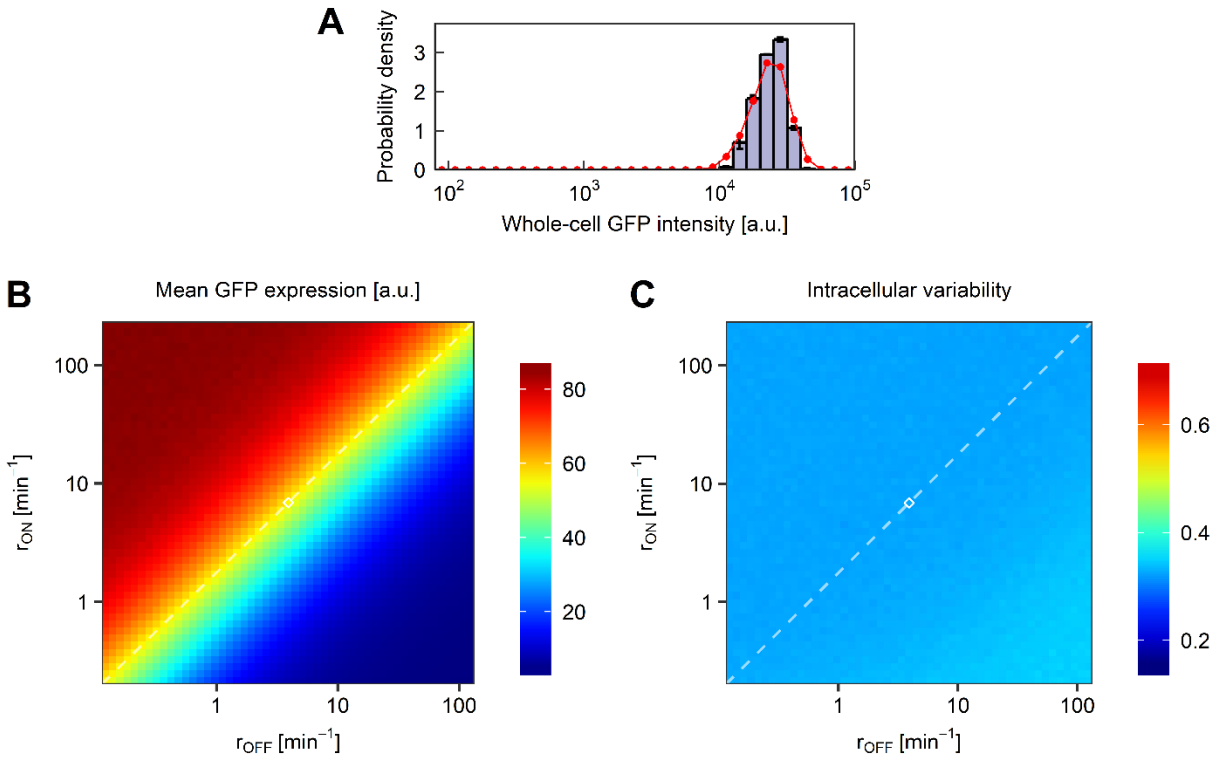

Figure S5. Model results for the homozygous P_{TEF1}-eGFP at *HIS3* locus strain. Related to Figure 8. **A.** Comparison of fit results (red) and experimental data for the homozygous P_{TEF1}-eGFP at *HIS3* locus strain. Error bars indicate s.e.m. (N=2). **B-C.** Effects of changes in r_{ON} and r_{OFF} on the mean expression level (**B**) and intracellular variability as measured by the coefficient of variation (**C**). White diamond indicates the fitted r_{ON} and r_{OFF} values. Dashed line indicates the result of simultaneous changes in r_{OFF} and r_{ON}.

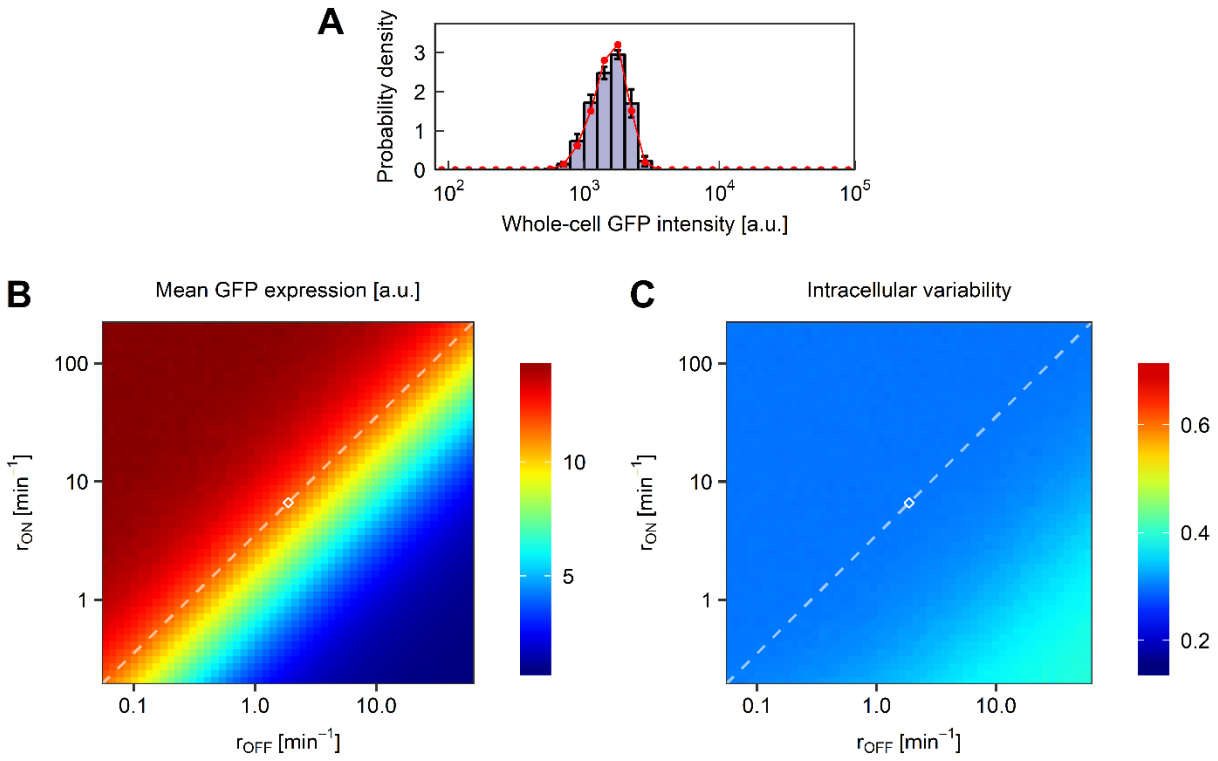

Figure S6. Model results for the homozygous P_{PGK1}-ssGFP at *HIS3* locus strain. Related to Figure 7. **A.** Comparison of fit results (red) and experimental data for the homozygous P_{PGK1}-ssGFP at *HIS3* locus strain. Error bars indicate s.e.m. (N=2). **B-C.** Effects of changes in r_{ON} and r_{OFF} on the mean expression level (**B**) and intracellular variability as measured by the coefficient of variation (**C**). White diamond indicates the fitted r_{ON} and r_{OFF} values. Dashed line indicates the result of simultaneous changes in r_{OFF} and r_{ON}.

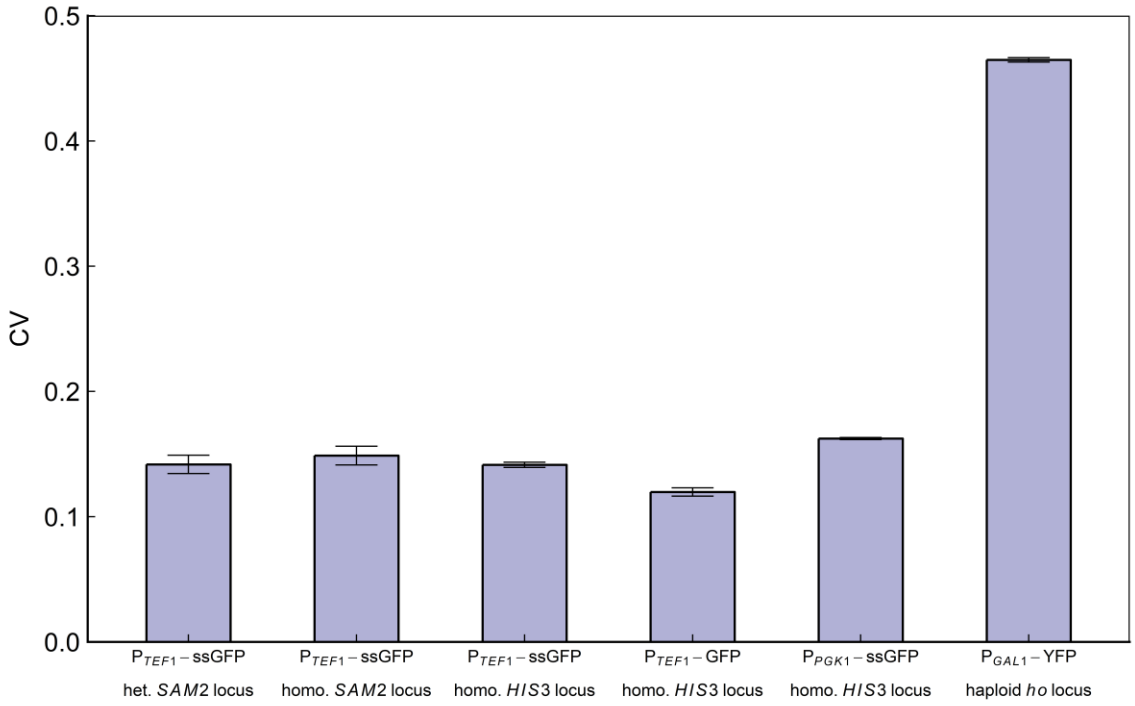

Figure S7. Comparison of population-level coefficients of variation between the five diploid strains under study and the P_{GAL1}-YFP haploid strain used in our previous work (Liu et al., 2017). Related to Figures 4-8. Error bars indicate s.e.m. (N=2).

SUPPLEMENTAL TABLES

Strain Description	Mean Lifespan
BY4743	30.44
BY4743	28.54
BY4743	28.06
BY4743 heterozygous for pTEF1-ssGFP at the SAM2 locus	28.51
BY4743 homozygous for pTEF1-ssGFP at the SAM2 locus	29.16
BY4743 homozygous for pTEF1-ssGFP at the HIS3 locus	29.46
BY4743 homozygous for pPGK1-ssGFP at the HIS3 locus	27.83
BY4743 homozygous for pTEF1-eGFP at the HIS3 locus	28.88

Table S1. Strains used and their mean lifespan characteristics. Related to Figure 1.

Parameter	Meaning	Value	Unit
mean and SD of r_1	Growth rate, G1	0.5 ± 0.125	fL min^{-1}
mean and SD of r_2	Growth rate, S/G2/M, total	1.5 ± 0.33	fL min^{-1}
mean and SD of r_{2m}	Growth rate, S/G2/M, mother compartment	0	fL min^{-1}
mean and SD of *T1'*	Minimum time before *start* for mothers	5 ± 2.5	min
mean and SD of *T2*	Time between *start* and S phase entry	5 ± 1.5	min
mean and SD of *T3*	Duration of S/G2/M	50 ± 5.78	min
mean and SD of V_i	Initial volume	75 ± 15	fL
k	Constants relating volume at *start* with r_1	160	min
b		24.0	fL
c	Level of inheritance for daughters	0.25	

Table S2. Parameters for the volume module. Related to Figures 4-8.

Parameter	Meaning	Value	Unit	References & Notes
r'_m	Apparent maximum transcription rate	2	min^{-1}	[Note A] [Note D]
r_p	Translation rate	1	min^{-1}	[Note A]
d_m	Degradation rate, mRNA	0.0346	min^{-1}	[Note A]
$d_{p,\ ssGFP}$	Degradation rate, ssGFP	0.00823	min^{-1}	[Note B]
$d_{p,\ eGFP}$	Degradation rate, eGFP	0.00101	min^{-1}	[Note B]
V_{ref}	Average volume of entire population	122	fL	[Note C]

Table S3. Fixed parameters for the gene network module. Related to Figures 4-8.

[Note A] Arbitrarily assigned. Any inaccuracy is accounted for during the fluorescence fitting process. To further improve generality, the additional initial conditions used (see Supplementary Text) have different values for these parameters.

[Note B] Calculated based on degradation data (Fig. 3).

[Note C] Assigned based on the results from running the volume model.

[Note D] Applicable to P_{TEF1} promoter in *SAM2* locus only. It is assumed that the actual transcription rate from the ON and OFF state promoter do not change with locus.

However, changes in the maximum fraction of time the promoter is in the ON state will lead to changes in the apparent maximum transcription rate (defined as the transcription rate measured at full induction).

Parameter	Meaning	Fitted value	Unit	Initial value	Lower bound	Upper bound
r_{ON}	Maximum OFF-to-ON transition rate	5.843	min^{-1}	1	0.01	10
f_{ON}	Fraction of time the promoter is in the ON state	0.7769		0.01	0.01	0.99
b'	Apparent basal expression level	0.0555		0.1	0	1
u_{ssGFP}	Fluorescence (a.u.) per ssGFP protein	0.6094		1	0.0001	10000
s	Volume noise scaling parameter	1.0424		0.25	0.01	2

Table S4. Fitted parameters for heterozygous P_{TEF1}-ssGFP in *SAM2* locus. Related to Figures 4 and 5.

Parameter	Meaning	Fitted value	Unit	Initial value	Lower bound	Upper bound
r_{ON}	Maximum OFF-to-ON transition rate	6.8803	min^{-1}	5.843	0.01	10
f_{ON}	Fraction of time the promoter is in the ON state	0.6379		0.7769	0.01	0.99

Table S5. Fitted parameters for homozygous P_{TEF1}-ssGFP in *HIS3* locus. Related to Figures 6 and 8.

Parameter	Meaning	Fitted value	Unit	Initial value	Lower bound	Upper bound
u_{eGFP}	Fluorescence (a.u.) per eGFP protein	1.88228		1	0.0001	10000

Table S6. Fitted parameters for homozygous P_{TEF1}-eGFP in *HIS3* locus. Related to Figure 8.

Parameter	Meaning	Fitted value	Unit	Initial value	Lower bound	Upper bound
r_{ON}	Maximum OFF-to-ON transition rate	6.6194	min^{-1}	5.843	0.01	10
f_{ON}	Fraction of time the promoter is in the ON state	0.7790		0.7769	0.01	0.99
b'	Apparent basal expression level	0.0793		0.0555	0	1
r'_m	Apparent maximum transcription rate	0.5710	min^{-1}	2	0.01	10

Table S7. Fitted parameters for homozygous P_{PGK1}-ssGFP in *HIS3* locus. Related to Figure 7.

TRANSPARENT METHODS

Yeast Strains, Media, and Culture Conditions

All experiments were conducted in a BY4743 strain background. Strains containing genetic modifications were constructed using lithium acetate transformation (Gietz and Schiestl, 2007). One or two copies of the specific [Promoter-Reporter-Terminator] cassettes were integrated in specific genomic loci in diploid yeast. Complete supplement mixture (CSM 2% glucose) was used as the media in all experiments. Media was prepared from powdered stock solutions fresh for each experiment. Cells were cultured in aerobic conditions and maintained at 30 °C in 50 mL conical tubes (Becton Dickinson F2070). All cultures were performed in an Innova-42 shaker (New Brunswick Scientific) at 225 rpm.

Design of the Duplicator

We aimed to create a device that would enable an automated microscope to image hundreds of diploid *S. cerevisiae* throughout the duration of their full RLS. A microfluidic channel containing structures designed to trap single cells is created between a soft plastic mold and a flat glass coverslip. Cells in culture media are introduced via an inlet and flow through the microfluidic channel into a waste container (Fig. 1A). Cells are tracked during aging by starting from their first generation; this is facilitated by having initially-loaded cells bud newborn daughters into the confines of a trap (Fig. 1B). Media is then flowed across the device for the duration of the experiment to wash daughter cells away and provide fresh nutrients. The Duplicator is mounted on an automated microscope, which images specified locations within the microfluidic chamber at regular intervals. This process generates a series of time-lapse images in which many cells can be observed from birth to death (Fig. 1C and Movie S1). The Duplicator was designed such that 16 separate channels could be affixed to a single 43 x 50 mm coverslip, each permitting observation of a different strain background or media condition.

Production of the Duplicator

The Duplicator is prepared by the joining of a glass coverslip and a PDMS cast prepared from a silicon wafer master mold. To prepare the mold, a silicon wafer with a 300 nm layer of thermal oxide (University Wafer #1583) was first coated in ZEP520A by spinning to equilibrium at 2000 rpm and baked at 180 °C for 5 minutes. The pattern of the microfluidic device was written into the resist with an electron beam lithography tool (EBPG, Raith), and developed by immersion in 0 °C xylenes for 20 seconds. The oxide layer was then etched using CHF_3 plasma in an Oxford Plasmalab 100 Reactive Ion Etching System. Next, the silicon was etched to a depth of 6 μm

using an Oxford Plasmalab 180 Reactive Ion Etching system set to cycle between SF_6 plasma and CHF_8 plasma. Finally, the remaining oxide was removed using CHF_3 plasma in the Oxford Plasmalab 100, and the wafer was washed thoroughly with water and dried with nitrogen gas.

To prepare the PDMS cast, the wafer mold was first placed into a small dish constructed of tight-fitting aluminum foil. This assembly was placed under vacuum adjacent to several drops of trichlorosilane (Sigma #448931) in a foil bowl for 20 minutes to vapor-coat the wafer. Afterward, a mixture of PDMS elastomer and curing agent (Dow Corning Sylgard 184 Silicone Elastomer Kit) was prepared in a 10:1 mass ratio totaling 44 g, and poured onto the surface of the wafer. The wafer was placed under vacuum for several hours until fully debubbled, and heated at 150 °C for 20 minutes to cure the PDMS. After cooling to room temperature, the PDMS was cut from the wafer with a sharp blade. Two inlet and one outlet holes were punched in each lane of the microfluidic device using a Schmidt Press (Syneo). The PDMS was thoroughly cleaned with isopropanol and dried. Finally, the PDMS was bonded to a clean 43 x 50 mm glass slide (Gold Seal #3329) using a corona treater (Electro-Technic Part 085-0057-3 BD-20ACV).

Performance validation for the Duplicator

Our first objective was to assess the reproducibility of results obtained from our device. We conducted three identical experiments in which we loaded cells to the device, and for 120 hours imaged 20 locations at 10-minute intervals. For each experiment, we assessed the lifespan of 50 wild-type cells (Fig. S1A). The mean$\pm$s.e.m. lifespan for cells from all three experiments was 29.0$\pm$0.7 generations, with mean values for each individual experiment falling within 5% of the overall mean value. This RLS approximates published values for the diploid BY4743 strain used in these experiments (Delaney et al., 2013; Yang et al., 2011).

In addition to lifespan, we investigated the retention rate of cells that became trapped in the device. For each of the experiments above, we noted the number of newborn cells that entered a trap, but escaped prior to their death. We found that 61% - 76% of the newborn cells that entered a trap and budded at least once could be observed for the duration of their lifespan (Fig. S1B). While this value is less than the 98% retention rate of the Replicator, we find that it is sufficient to measure lifespan for approximately 100 cells in each lane of the device (Fig. S1C). The retention rate of the Duplicator could be further increased by slightly decreasing the area of the trapping units in the device. However, we opted against it as such a decrease would hamper the precision of the measurements for cellular area and perimeter.

Duplicator Experiments

18” of tubing (Cole-Parmer 06419-00) was connected to the outlet and cell inlet of each Duplicator lane. 12” of the same tubing was connected to the media inlet. The media inlet was connected to a 250 mL flask (Duran 10-922-34) attached to a digital pressure regulator (Fluigent MFCS). Media was introduced to the device at a pressure of 100 mbar, and the cell inlet was stoppered with an insect pin. The traps within the channel were debonded from the glass slide by increasing pressures of up to 1900 mbar. Cells were cultured for 18 hours to an approximate OD_{600nm} of 0.7, and introduced via the cell inlet at a rate of 10 µL/minute using a syringe pump (New Era Pump Systems Inc., NE-1000) with media pressure set to 100 mbar. After loading, the cell inlet was backflushed with media at 130 mbar for 30 minutes to remove all cells from the inlet tubing, where their growth would create clogging in the microfluidic device. During the flush, an automated microscope was used to select 20 imaging locations within each lane of the microfluidic device. The right-most traps were avoided, as those too close to the outlet experienced a high rate of cell loss. After the flush, media pressure was set to 100 mbar, and the cell inlet tubing was clamped shut with a 1” binder clip. The automated microscope was set to image the device at regular intervals, typically of 10 minutes, for 120 hours. Media pressure was set to oscillate and increase over time to prevent clogging of the device as aged, enlarged cells became more prevalent in the population.

Measurements in the Duplicator Device

RLS was scored manually by observing the time-lapse image series produced in a Duplicator experiment. Cells were included for measurement if they completed at least one budding cycle while alone in the trap prior to the 12th hour of the experiment. Passage into each generation was denoted by the appearance of a bud. The results of all RLS measurements are shown in Supplementary Table S1. Fluorescence and area measurements were made using the Bezier circling tool of the NIS Elements Advanced Research software. Fluorescence measurements used for analysis and graphing were first subjected to background subtraction with the average GFP intensity for 10 wild-type cells throughout their lifespan.

Estimation of Cell Volume

The area and perimeter of cells was measured at hourly intervals, simultaneous to the measurement of fluorescence intensity. We assumed that diploid yeast could be approximated as ellipsoid. Therefore, cell volume is defined by the formula $Volume = \frac{4}{3}\pi a^2 b$ where a represents the radius along the short axis, and b is the radius of the long axis. Working from a 2-dimensional

image taken at the center of the ellipse, we set $a+b=\sqrt{2\frac{Perimeter^2}{2\pi}+\frac{Area}{\pi}}$ and $a-b=\sqrt{2\frac{Perimeter^2}{2\pi}-\frac{Area}{\pi}}$, then solved for a and b. In the rare instance that $a^2<b$, our equations were invalid. These data points were omitted.

Flow Cytometry

All measurements were performed using a BD FACSVerse, with cells grown for 18 hours to mid-log phase, an OD_{600} of 0.1-1, at the start of the experiment. For half-life measurements, cycloheximide (Sigma C4859) was added to each culture to a concentration of 10 µg/mL. The cultures were then returned to the shaking incubator, with aliquots taken every 10 minutes for flow cytometry. For other modeling measurements, cultures were placed on ice after 18 hours, then immediately used for flow cytometry.

Description of the Stochastic Model

We adapted our previously described stochastic model (Liu et al., 2017) to the expression of ssGFP and GFP from the TEF1 and PGK1 promoters. Briefly, the promoter is assumed to stochastically switch between two states, OFF and ON. Transcription occurs at the basal rate in the OFF state and at the maximal rate in the ON state. The resultant mRNA is translated to produce the fluorescent reporter, and both protein and mRNA can be degraded.

Volume and cell cycle is controlled by a separate volume module based on previous work (Ferrezuelo et al., 2012). The cell cycle is divided into two parts: G1 and S/G2/M, with the volume increasing linearly, but at different rates, in each part of the cell cycle. The G1 phase growth rate (an independent variable) is linearly related to the volume at which the cell enters S, with a separate floor on G1 phase duration so that mother cells do not immediately reenter S. We fixed the volume module parameters to be generally consistent with our experimental measurements (Fig. 2, Table S2). Protein degradation rates were fixed based on our measurements, and other parameters related to mRNA and protein synthesis and mRNA degradation were fixed from general ranges reported in literature (Table S3).

In each case, experimental data was obtained by flow cytometry. The model was fitted to the data using the same procedure as previously described (Liu et al., 2017). To summarize, a population of 25,000 freely dividing cells were simulated with resampling every 40 minutes to keep the population size approximately constant. At the end of the simulation, the reporter protein (ssGFP) level in each cell is converted to a simulated fluorescence level and a simulated

fluorescence distribution is obtained. The Nelder-Mead algorithm (Nelder and Mead, 1965), as implemented in the NLopt (Johnson, 2014) library, is used to find parameter values that maximize the likelihood of observing the experimental distribution.

To determine the effects of the promoter dynamics parameters r_{ON} and r_{OFF} on intracellular expression variability, we systematically varied each in a wide range (between 10% and 1000% of the fitted value). An initial population of 20,000 exponentially growing cells were simulated for 24 hours with periodic resampling to ensure that they have reached steady state, and then 5,000 cells were randomly sampled from the population and simulated for another 40 generations. In this second stage, only the 5,000 cells themselves are considered (daughters are discarded), and the reporter protein expression level in each cell is recorded every 10 minutes and used to calculate the intracellular variability level for each cell (expressed as the coefficient of variation). The calculated intracellular variability level for all 5000 cells are then averaged to produce an intracellular variability value for the entire population.

Heterozygous P_{TEF1}-ssGFP, *SAM2* locus

We determined the fitted parameter values for this strain and the conversion factor from ssGFP to simulated fluorescence by fitting the simulation output to the experimentally observed distribution (Table S4). The results are shown in Figure S2. Simultaneous changes in the values of r_{ON} and r_{OFF} as we previously postulated for P_{GAL1} in haploid cells (Liu et al., 2017) has minimal effects on the level of intracellular variability for this promoter.

Homozygous P_{TEF1}-ssGFP, *SAM2* locus

We performed simulations for the homozygous case by using the same fitted parameters for the heterozygous case, merely increasing the number of copies of the gene in the model from 1 to 2. The results are shown in Figure S3 and are extremely similar to the heterozygous strain after accounting for the roughly doubled level of expression.

Homozygous P_{TEF1}-ssGFP, *HIS3* locus

We fitted the promoter dynamics parameters of this strain to account for the different locus (Table S5), keeping all other parameters at the same value. The results are shown in Figure S4 and are also quite similar to the previous ones except for the expression level difference.

Homozygous P_{TEF1}-eGFP, *HIS3* locus

The degradation rate difference alone cannot explain the 5-fold difference in the experimentally observed mean fluorescence levels of the ssGFP and eGFP strains. We therefore postulated that

the additional tag may have also made ssGFP less bright than eGFP, and fitted the fluorescence conversion factor of eGFP for this strain (Table S6), keeping all other parameters at the same value. The results are shown in Figure S5 and are once again quite similar to the previous strains.

Homozygous P_{PGK1}-ssGFP, *HIS3* locus

We fitted the promoter dynamics and transcription parameters of this strain to account for the different promoter (Table S7), keeping all other parameters at the same value. The results are shown in Figure S6 and are also quite similar to the previous ones except for the expression level difference.

Different initial conditions

For each of these 5 strains, we also repeated the entire analysis for 9 additional sets of initial conditions. The results are not materially different: in all cases, the intracellular noise value is not substantially affected by increases in the promoter dynamics parameters, indicating that the two constitutive promoters under study are already at the "noise floor" such that the potential for additional noise reduction is minimal.

Different doubling times

Because the single-cell level doubling time was experimentally observed to vary over time as the cell ages, we further repeated the analysis for four separate doubling time values (80 minutes, 120 minutes, 160 minutes and 200 minutes) for all strains and initial conditions. We observed a minor decrease in intracellular variability levels from increasing the doubling time, which is due to increases in the reporter protein concentration (as expected due to reduced dilution).

Experimental observations are consistent with "noise floor"

We computed the population-level coefficients of variation of GFP fluorescence (as measured by flow cytometry) for all five strains and compared them to the CV calculated for the haploid *gal80Δ* strain carrying P_{GAL1}-YFP in *ho* locus. As can been seen from Figure S7, all five strains have substantially less intercellular variability than the haploid P_{GAL1}-YFP strain, with the CV values being roughly one-third of that strain. This corroborates our hypothesis that the five diploid strains are at the "noise floor" with little room for further reduction.

SUPPLEMENTAL REFERENCES

Gietz, R.D., and Schiestl, R.H. (2007). High-efficiency yeast transformation using the LiAc/SS carrier DNA/PEG method. Nat. Protoc. *2*, 31–34.

Johnson, S.G. (2014). The NLopt nonlinear-optimization package.

Nelder, J.A., and Mead, R. (1965). A Simplex Method for Function Minimization. Comput. J. *7*, 308–313.